Partial-Wave Analysis of the Inelastic Scattering of Electrons by Nuclei. III. Systematics of Electric Multipole Excitation*

D. S. ONLEY, J. T. REYNOLDS,† AND L. E. WRIGHT‡
Physics Department, Duke University, Durham, North Carolina
(Received 17 January 1964)

The distorted-wave method for inelastic electron scattering is applied to a range of nuclei displaying electric multipole excitations under electron bombardment. It is found that a phenomenological vibrator model of the nucleus can, to a large extent, account for the behavior of the electron inelastic cross sections available from experiment, although, in many cases, the measured points cover an insufficient range of momentum transfer to make distinct the mode of vibration to be attributed to the excited nucleus.

I. INTRODUCTION

IN two previous papers[1,2] (referred to as I and II in this text) a method for distorted-wave calculation of inelastic electron scattering from nuclei was proposed, and used to predict differential cross sections for electric quadrupole excitations of target nuclei. In II a simple phenomenological model of electric excitations was shown to give a fair description of existing data on electron stimulated quadrupole excitations. In the present paper (in Sec. II) the extension of this technique to higher multipole excitations is discussed, and (in Sec. III) some general observations are made on the introduction of distorted waves as compared with the plane-wave Born approximation. Data on several nuclei which show a number of electric multipole excitations in electron scattering experiments, are examined in Sec. IV and values are given of the transition probabilities necessary to account for the observed magnitude of the cross section in each case. Where some ambiguity as to the correct multipolarity to be assigned to a given transition is apparent, it is suggested (in Sec. V) that measurements at low-momentum transfer (incident energies around 50 MeV and forward angles) would be valuable. Finally (in Sec. VI) conclusions and comments are presented on the usefulness of excitation by electrons as a probe of nuclear excited states.

II. DESCRIPTION OF VIBRATIONAL STATES

The transition is described, following I and II, by means of a transition charge density $\rho_{\text{trans}}(\mathbf{r})$ which characterizes the contribution of the nuclear transition to the scalar part of the electromagnetic interaction between the electron and the nucleus. An argument is presented in the Appendix indicating the conditions under which the sum effect of longitudinal and transverse electric-interaction terms can be neglected. For an electric multipole transition of order L and energy $\hbar\omega$ we may write

$$\rho_{\text{trans}}(\mathbf{r})=\rho_L(r)Y_L{}^M(\theta,\varphi)e^{i\omega t}, \tag{1}$$

where the radial part $\rho_L(r)$ is, in principle, subject to determination from study of electron excitation of this state just as the ground-state charge distribution $\rho_0(r)$ may be determined from elastic electron scattering. The actual extraction of $\rho_L(r)$ from the measured cross section is not a simple matter in the distorted-wave theory used in this paper, but it is noted that the transition charge density enters the calculation only through the cutoff function[3] $C(r)$ and this is quite insensitive to the behavior of the transition charge density near the origin. The surface features will therefore dominate the scattering unless incident energies in the BeV region ($E_e \gg \hbar c/a$, where a is the nuclear radius) are used. It is not surprising therefore, that as far as the inelastic scattering is concerned, the form of $\rho_L(r)$ is well represented by a peak at the nuclear surface[4]; but what is interesting is the possibility of relating this form to the ground-state distribution in a simple fashion. Therefore a model has been adopted in which the transition charge distribution is "tied" to the ground-state distribution by treating it as a distortion of $\rho_0(r)$. There is considerable latitude here, both in the mode of distortion assumed and in the choice of the shape of $\rho_0(r)$ (which must however conform to a given half-density radius a and diffuseness t, as defined by Hofstadter[5]). Three expressions for $\rho_L(r)$ have been used in this work, two of which take the Fermi shape,

$$\rho_F(r)=\rho_0\Big/\left[1+\exp\left(\frac{r-a}{z_1}\right)\right], \tag{2}$$

for the ground state, where $t=4.4z_1$, but differ in the mode of distortion. Explicitly:

$$\rho_L{}^{(1)}(r)=\beta_L r^{L-1}(d\rho_F/dr) \tag{3}$$

and

$$\rho_L{}^{(2)}(r)=\beta_L r(d\rho_F/dr), \tag{4}$$

where the first is the result of assuming incompressible

* Supported in part by the U. S. Army Research Office (Durham) and the National Science Foundation.
† National Science Foundation Cooperative Fellow.
‡ DuPont Teaching Assistant.
[1] T. A. Griffy, D. S. Onley, J. T. Reynolds, and L. C. Biedenharn, Phys. Rev. **128**, 833 (1962).
[2] D. S. Onley, T. A. Griffy, and J. T. Reynolds, Phys. Rev. **129**, 1689 (1963).
[3] See Appendix, Eq. (A22).
[4] See, for example, R. Helm, Phys. Rev. **104**, 1466 (1956).
[5] R. Hofstadter, Ann. Rev. Nucl. Sci. **7**, 231 (1957).

and irrotational fluid flow and the second would result from giving the ground-state distribution a uniform radial strain. Modes 1 and 2 become identical for quadrupole transitions and this case was discussed in II. A third mode is obtained by taking a different function for $\rho_0(r)$, namely,

$$\rho_1(r)=\rho_0\{1-\exp[-((r-c)/d)^2]\}, \quad \text{for } r<c$$
$$=0, \quad \text{for } r>c, \tag{5}$$

where the choice $d=3.7z_1$ and $c=a+3.1z_1$ gives the same a and t as the Fermi shape. Mode 3 is then defined to be

$$\rho_L^{(3)}(r)=\beta_L r^{L-1}(d\rho_1/dr). \tag{6}$$

It is clear that these modes claim no special distinction on dynamical grounds but merely serve as prescriptions in our attempt to demonstrate that the transition charge density is essentially governed by the same parameters as the ground-state density. The third parameter β_L governs the over-all normalization of the cross section and this may be determined by fitting to the experimental cross section. The result is then expressed in terms of the reduced transition probability

$$B(EL)=(2L+1)\left(\int r^L\rho_L(r)r^2dr\right)^2. \tag{7}$$

III. THE DISTORTED-WAVE CALCULATIONS

In order to take account of the distortion of the incident-electron wave function by the static Coulomb field of the nucleus, the method of partial-wave analysis of the Dirac equation in a central field has been used, as described in I. A brief resumé of this method and discussion of the approximations applied in the present calculations are given in the Appendix. Some general observarions on the effect of the Coulomb field are made here, which are intended to apply to electrons above 100 MeV (i.e., of sufficiently high energy to reveal something about nuclear structure). For this purpose it is convenient to distinguish nuclei of "medium" charge (say $Z<40$) from the "heavy" group ($Z>40$). In the medium group it is possible to describe the behavior of the differential cross section, at least for scattering in the forward hemisphere,[6] in terms of a modification of the Born approximation. The lowest order effect of the potential is to contract the electron wavelength near the nuclear surface or, equivalently, to produce an apparent dilation in the size of the nucleus of order $\alpha Z/E_e$ (α is the fine structure constant and E_e the incident electron energy). As a result the Born approximation cross-section curve should be shifted to the left (smaller angles) for electrons and to the right for positrons; this is evident from Fig. 1 in which the distorted-wave calculations for 187-MeV electrons and positrons scattering from Sr^{88} are compared with the Born approximation. An example of the behavior of this correction as a function of Z is shown in Fig. 2; this curve is not intended to be precise since the criterion for determining the correction is, itself, imprecise. It is also clear from Fig. 1 that the *peak* value of the relative cross section $\sigma(\theta)/\sigma_{\text{Mott}}(\theta)$ is unchanged by the introduction of distorted waves. This holds even for large distortion as in the case of electron scattering from Pb^{208}, shown in Fig. 3, although here the departure from the diffraction shape of the Born approximation is manifest.

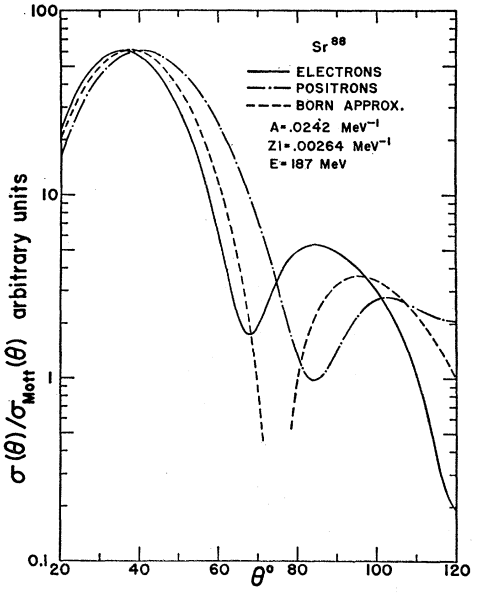

FIG. 1. Relative cross sections for 187-MeV electrons and positrons scattered from Sr^{88} with an $E2$ excitation compared with the corresponding Born approximation.

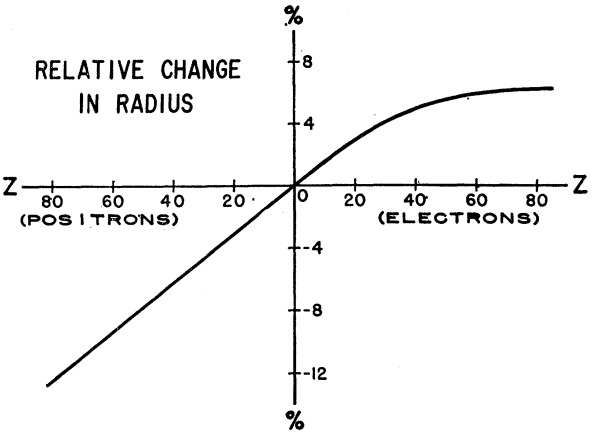

FIG. 2. Change in nuclear radius needed to correct Born approximation cross section for $L=2$ as a function of Z. Negative Z corresponds to positrons.

[6] This appears to be independent of energy and of the multipole order of the transition. It is evident that for higher incident energies the cross section becomes more "Born-like" over a wider range of momentum transfer, but this range still corresponds to forward scattering.

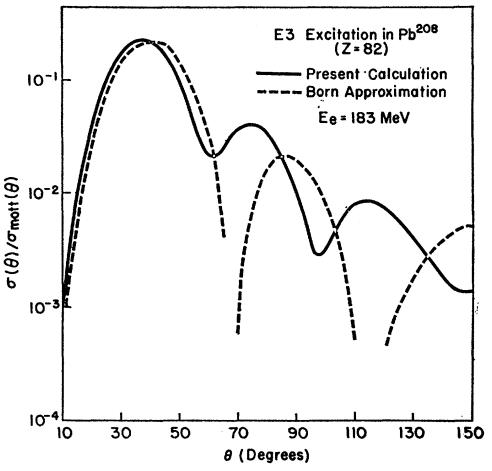

FIG. 3. Relative cross section for an $E3$ excitation in Pb^{208} compared with the corresponding Born approximation.

IV. COMPARISON WITH EXPERIMENT

Available data[7] in the medium charge region are most complete for the nickel isotopes. Ni^{58} shows electron induced excitations at 1.45, 2.5, 3.2, 3.5, 4.5, and 7.55 MeV and Ni^{60} at 1.33, 2.50, 4.05, and 5.1 MeV. Those at approximately 1.4, 2.5, and 4.1 MeV probably correspond in the two nuclei and have fairly well-established spins (2^+, 4^+, 3^-, respectively). The data of the last two of these have been compared with the predictions of the distorted-wave calculation using both mode 1 and mode 2 [Eqs. (3) and (4)]. The results are shown, together with the corresponding levels in Co^{59}, in Figs. 4 and 5. (Similar comparisons for the levels around 1.4 MeV were shown in II to be satisfactorily interpreted as $E2$ excitations.) For the octupole case the features of the angular distribution seem to be well represented by mode 2 at angles less than 65°. The enhanced cross section beyond 65° could be suggestive of additional structure in the transition charge distribution inside the nuclear surface which our model is not designed to take into account. The $E4$ case does not show sufficient consistency among the three nuclei to admit any definite comment beyond the observation that mode 2 is adequate. The third mode [Eq. (6)] is not shown, but gives a curve whose shape is little distinguished from mode 2 in this range but in magnitude is considerably larger, and hence, while being an equally good fit to the data, requires a value of $B(EL)$ which is considerably smaller than that required by mode 2 (see Table I for comparison). With this reservation on the value of the reduced transition probability, mode 2 has been used as the standard for all subsequent anaylses of nuclear transitions. Figures 6 and 7 show four levels in Cu^{63} reported by Kendall[8] and it is again remarkable that where points are shown beyond 70° they do not lie on the calculated curve.

Heavy nuclei are represented by the pair, Pb^{208} and

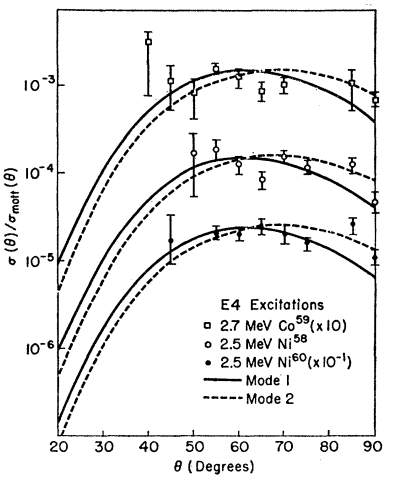

FIG. 5. Calculated relative cross sections for $E4$ excitations in Ni^{58}, Ni^{60}, and Co^{59}.

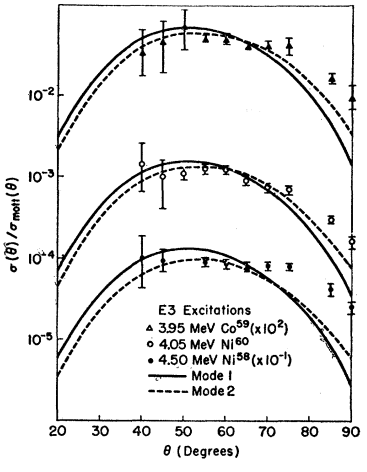

FIG. 4. Calculated relative cross sections for $E3$ excitations in Ni^{58}, Ni^{60}, and Co^{59}. Modes 1 and 2 are specified in the text. The data points for Figs. 4 and 5 are taken from Ref. 7.

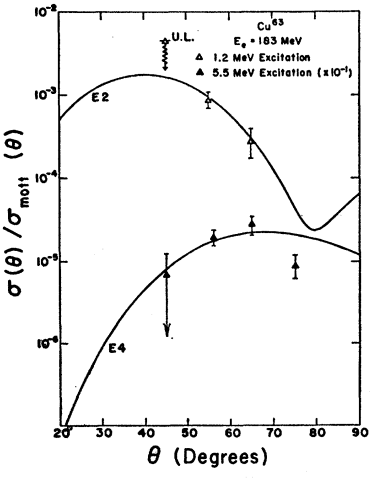

FIG. 6. Calculated relative cross sections for $E2$ and $E4$ excitations in Cu^{63}. The data points for Figs. 6 and 7 are taken from Ref. 8.

[7] H. Crannell, R. Helm, H. Kendall, J. Oeser, and M. Yearian, Phys. Rev. **123**, 923 (1961).

[8] H. W. Kendall and Jan Oeser, Phys. Rev. **130**, 245 (1963).

TABLE I. Values of the reduced transition probability for electron induced electric multipole transitions. Experimental data are taken from Refs. 4, 7, and 8. For explanation of "Mode" see Sec. II.

Nucleus	Transition energy (MeV)	Multipolarity (L)	$[B(EL)/e^2]$ (F^{2L})	Mode
Ni^{58}	1.45	2	1.66×10^3	2
			9.3×10^2	3
	2.50	4	2.18×10^5	2
			1.04×10^5	3
	4.50	3	2.70×10^4	2
			1.61×10^4	3
Co^{59}	1.30	2	1.14×10^3	2
	2.70	4	2.07×10^5	2
	3.95	3	1.56×10^4	2
Ni^{60}	1.33	2	1.74×10^3	2
	2.50	4	3.58×10^5	2
	4.05	3	3.59×10^4	2
Cu^{63}	1.2	2	9.50×10^2	2
	2.6	3	1.50×10^4	2
	3.6	3	2.03×10^4	2
	5.5	4	3.05×10^5	2
Sr^{88}	1.85	2	1.00×10^3	2
	2.76	3	4.78×10^4	2
Pb^{208}	2.60	3	8.8×10^5	2
	4.30	2	1.63×10^4	2
		4	4.08×10^7	2
	5.8	3	6.36×10^5	2
		5	7.74×10^8	2
Bi^{209}	2.60	3	9.42×10^5	2
	4.30	2	1.73×10^4	2
		4	3.90×10^7	2

Bi^{209}, which have levels in common at 2.6 and 4.3 MeV of which the first is known to be[9] $E3$ and the second is thought to be[7,8] $E4$. This calculation supports the $E3$ identification of the 2.6-MeV level (Fig. 8) but does not produce a convincing $E4$ fit to the electron scattering data on the 4.3-MeV excitation (Fig. 9). The data on Bi^{209} show a clear preference for $E2$ whereas the corresponding level in Pb^{208} admits an $E2$, $E4$, or less likely,

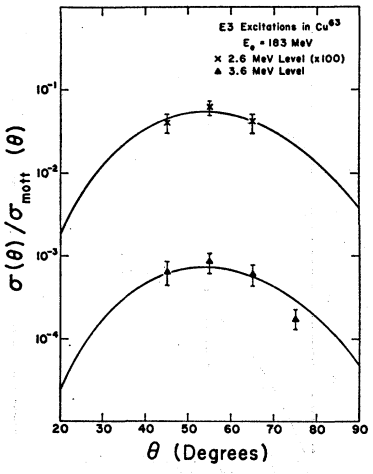

FIG. 7. Calculated relative cross sections for $E3$ excitations in Cu^{63}.

[9] See *Nuclear Data Sheets*, compiled by K. Way *et al.* (Printing and Publishing Office, National Academy of Science–National Research Council, Washington 25, D. C.), NRC 61-3-127.

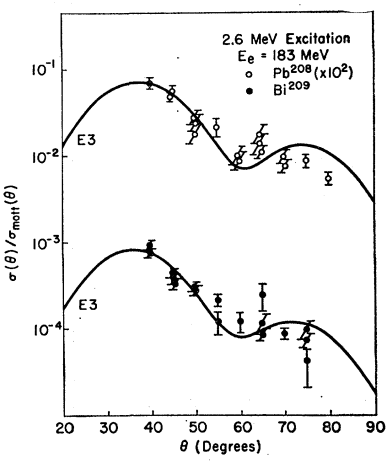

FIG. 8. Calculated relative cross sections for $E3$ excitations in Pb^{208} and Bi^{209}. The data points for Figs. 8 and 9 are taken from Ref. 7.

$E3$ interpretation. A distinction among these choices could be made if data at low-momentum transfers were available. A similar situation occurs for the 5.8-MeV level in Pb^{208} also reported by Kendall[8] and shown in Fig. 10. In this case, the more conservative $E3$ interpretation would be tenable if the cross section were known to be large around 30°. As it stands the $E5$ curve deviates from the measured points only beyond the 70° point, and therefore cannot be ruled out.

V. INELASTIC SCATTERING AT LOW ENERGIES

In the examples cited in the previous section where the multipolarity of a transition is in doubt, the question could be settled if the scattering at low-momentum transfers were known. In fact the examination of the nuclear structure would be more fruitful, if independent measurements could be made of both the multipolarity L, and the reduced transition probability $B(EL)$. But these quantities should be precisely the governing factors of the behavior of inelastic electron scattering at low-momentum transfer where the cross section is insensitive to the details of the nuclear structure. The Born approximation calculation has the well-known

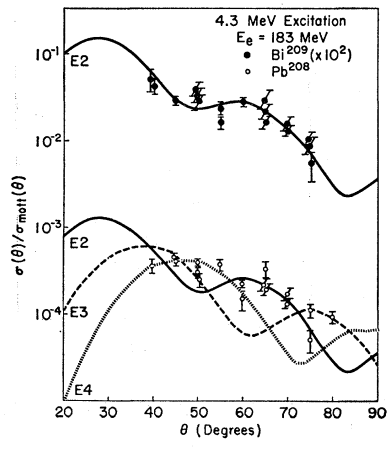

FIG. 9. The 4.3-MeV levels in Pb^{208} and Bi^{209}. The calculated curves shown are the "preferred fits."

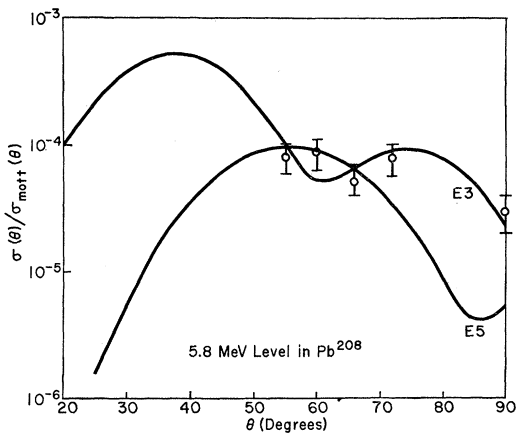

FIG. 10. The 5.8-MeV level in Pb^{208}. The data points are taken from Ref. 8. The calculated curves shown are the "preferred fits."

form[10]

$$\sigma(q)/\sigma_{\text{Mott}}(q)\cong 4\pi B(EL)[q^L/Ze(2L+1)!!]^2 \text{ as } q\to 0 \quad (8)$$

which is model-independent, as expected. There is, therefore, some interest attached to the question of whether a comparable relation emerges from the distorted-wave treatment, particularly because measurements in this region would have to be made at low incident electron energy where the distortion is greatest. From the appearance of Figs. 1 and 3 it is evident that the electron cross section will be enhanced in this region but is not seriously changed in functional form; i.e.,

$$[\sigma(q)/\sigma_{\text{Mott}}(q)]_{\text{dist}}\cong\lambda(E_e)[\sigma(q)/\sigma_{\text{Mott}}(q)]_{\text{Born}}. \quad (9)$$

To display this, the calculated relative cross section at 50 MeV for scattering from Pb^{208} (where there is considerable distortion) has been plotted against q on a log-log scale in Fig. 11. The q^{2L} law still holds to a high degree of accuracy and should, in principle, afford a simple method for the extraction of both the multipolarity and reduced transition probability. If these data were available, many of the ambiguities of Table I could be resolved.

VI. CONCLUSIONS

The feasibility of determining the electromagnetic structure of excited nuclear states by electron scattering is not really in doubt. The foregoing examples show that the general behavior of the electron inelastic cross section can be accounted for by a pronounced peak in the transition charge distribution at the nuclear surface, derived from the ground-state charge distribution in the manner of Eq. (4), for example. This suggests that some of the spatial characteristics of the collective oscillation are already contained in the collective description of the ground state (e.g., its distribution of charge); whereas the energy and strength of any given level may well depend on the intricacies of nuclear structure. Comparison of electron-scattering data with nucleon-scattering data[11] suggests that the charge distribution follows the same general mode of deformation as that used in the corresponding nuclear potential well, to account for neutron and proton excitation of these levels. This, of course, is in accord with the idea of self-consistency. The full value of inelastic electron scattering lies in a consistent study covering a wide range of electron energies and angles (including low-energy scattering). This could provide a reconstruction of the structure of the excited state independent of any specific nuclear model which would then serve as a "constraint" on nuclear model treatments, in the same way as the knowledge of the ground-state charge distribution has helped in the determination of, for instance, the ground-state potential of the nuclear shell model.

Additional information on nuclear structure may be gained by analyzing electron-scattering data for magnetic multipole excitations and electric multipole excitations for scattering around 180°, and such calculations are in progress.

ACKNOWLEDGMENTS

The authors would like to express their thanks to Professor L. C. Biedenharn for his interest and encouragement, and their gratitude for the patience and help of the staff of the Duke University Computer Laboratory.

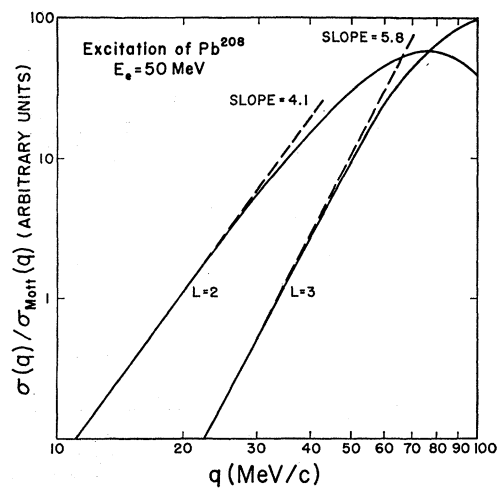

FIG. 11. Relative cross section for $E2$ and $E3$ excitations of Pb^{208} by 50-MeV electrons as a function of the momentum transfer q.

[10] L. I. Schiff, Phys. Rev. **96**, 765 (1954).

[11] For a review of work in this field see G. R. Satchler, in *Proceedings of the International Symposium on Direct Interactions and Nuclear Reactor Mechanism, Padua*, edited by E. Clementel and C. Villi (Gordon and Beach, New York, 1963), p. 80.

APPENDIX

A resumé of the distorted-wave treatment for electrons, and discussion of the approximations applied in this paper, are presented here.

The solutions of the Dirac equation for an electron of energy E, and mass m_e, in a central potential, $V(r)$, are well known and have the form[12]

$$\psi_\kappa{}^\mu(p,\mathbf{r})=\left\{\begin{array}{c} g_\kappa(p,r)\chi_\kappa{}^\mu(\hat{r}) \\ if_\kappa(p,r)\chi_{-\kappa}{}^\mu(\hat{r}) \end{array}\right\}, \tag{A1}$$

where $p^2=E^2-m_e{}^2$ (the convention $\hbar=c=1$ has been used throughout), and the angular momentum functions are given explicitly by

$$\chi_\kappa{}^\mu=\sum_\tau C_{\mu-\tau\tau\mu}{}^{l\frac{1}{2}j}Y_l{}^{\mu-\tau}(\hat{r})\chi^\tau. \tag{A2}$$

The radial functions, f_κ and g_κ, are solutions of the coupled differential equations

$$\begin{aligned}\frac{df_\kappa}{dr}&=\frac{\kappa-1}{r}f_\kappa-[E-m-V(r)]g_\kappa,\\ \frac{dg_\kappa}{dr}&=[E+m-V(r)]f_\kappa-\frac{\kappa+1}{r}g_\kappa.\end{aligned} \tag{A3}$$

The appropriate combination of the $\psi_\kappa{}^\mu$ to describe an incident distorted wave for an electron with energy, E_i, and momentum, $\mathbf{p}_i$, is

$$\psi_i{}^m=4\pi\left(\frac{E_i+m_e}{2E_iV}\right)^{1/2}\sum_{\kappa\mu}\exp(i\delta_\kappa)i^lC_{\mu-mm\mu}{}^{l\frac{1}{2}j}\times Y_l{}^{\mu-m*}(\hat{p}_i)\psi_\kappa{}^\mu(p_i,\mathbf{r}). \tag{A4}$$

Here, $m(=\pm\frac{1}{2})$ is the eigenvalue of the polarization operator,[12] O_z, V is the volume of normalization, and δ_κ is the phase shift of partial wave, κ. A similar wave function describes an outgoing distorted wave with energy and momentum, E_f, $\mathbf{p}_f$;

$$\psi_f{}^m=4\pi\left(\frac{E_f+m_e}{2E_fV}\right)^{1/2}\sum_{\kappa\mu}\exp(-i\bar{\delta}_\kappa)i^lC_{\mu-mm\mu}{}^{l\frac{1}{2}j}\times Y_l{}^{\mu-m*}(\hat{p}_f)\bar{\psi}_\kappa{}^\mu(p_f,\mathbf{r}). \tag{A5}$$

Here bars are added to δ_κ and $\psi_\kappa{}^\mu$ to denote the values of these in the final state [if the distorting potential, $V(r)$, is assumed to be unchanged in the final state the bars can be omitted].

The interaction Hamiltonian operator may be separated into scalar and vector parts in the form

$$H_{\rm int}=-4\pi\alpha[\rho_NG(\mathbf{r}_N,\mathbf{r}_e)\rho_e-\mathbf{j}_N\cdot G(\mathbf{r}_N,\mathbf{r}_e)\mathbf{j}_e], \tag{A6}$$

where α is the fine structure constant, ρ_N, $\mathbf{j}_N$, $(\rho_e,\mathbf{j}_e)$, are the change and current density operators for the nucleus (electron), and G is the Green's function:

$$G(\mathbf{r}_N,\mathbf{r}_e)=\frac{e^{i\omega|\mathbf{r}_N-\mathbf{r}_e|}}{4\pi|\mathbf{r}_N-\mathbf{r}_e|} \tag{A7}$$

expressed in terms of the electron coordinate, $\mathbf{r}_e$, and the collective nuclear coordinate, $\mathbf{r}_N$, where $\omega=E_i-E_f$, the energy transferred in the transition. Let $\Psi_i(I_i,M_i)$ and $\Psi_f(I_f,M_f)$ represent the initial and final nuclear wave functions, with I_i and M_i (I_f and M_f) the initial (final) angular quantum numbers. Then the transition amplitude is given by

$$A(M_i,M_f,m_i,m_f,\mathbf{p}_i,\mathbf{p}_f)=\langle\Psi_f(I_f,M_f)\psi_f{}^{m_f}|H_{\rm int}|\Psi_i(I_i,M_i)\psi_i{}^{m_i}\rangle. \tag{A8}$$

The evaluation of this requires the matrix elements for ρ and $\mathbf{j}$ which, for the electron, are explicitly

$$\rho_e(m_i,m_f,\mathbf{r}_e)=\psi_f{}^{m_f\dagger}\psi_i{}^{m_i}, \tag{A9}$$

$$\mathbf{j}_e(m_i,m_f,\mathbf{r}_e)=\psi_f{}^{m_f\dagger}\boldsymbol{\alpha}\psi_i{}^{m_i}, \tag{A10}$$

and, for the nucleus, are written as a multipole sum,

$$\rho_N(M_i,M_f,\mathbf{r}_N)=\sum_{LM}J_{LM}(M_i,M_f,r_N)Y_L{}^M(\hat{r}_N), \tag{A11}$$

$$\mathbf{j}_N(M_i,M_f,\mathbf{r}_N)=\sum_{JLM}I_{JLM}(M_i,M_f,r_N)\mathbf{Y}_{JL}{}^M(\hat{r}_N). \tag{A12}$$

the exact form of which depends on the nuclear model assumed. For electric multipole excitations A now appears in the form

$$A(M_i,M_f,m_i,m_f,\mathbf{p}_i,\mathbf{p}_f)=\sum_{LM}E_{LM}(M_i,M_f,m_i,m_f,\mathbf{p}_i,\mathbf{p}_f), \tag{A13}$$

where (for $\mathbf{p}_i=p_i\hat{z}$)

$$E_{LM}(M_i,M_f,m_i,m_f,\mathbf{p}_i,\mathbf{p}_f)=8\pi^2\alpha[(E_i+m_e)(E_f+m_e)/E_iE_fV^2]^{1/2}\times\sum_{\kappa,\kappa'}e^{i[\delta_\kappa+\delta_{\kappa'}]}i^{l-l'}(-)^{j'+L+l+\frac{1}{2}}(2l+1)[(2j+1)/(2L+1)]^{1/2}C_{0m_im_i}{}^{l\frac{1}{2}j}C_{m_i+M-m_fm_fm_i+M}{}^{l'\frac{1}{2}j'}C_{000}{}^{lL l'}\times C_{m_iMm_i+M}{}^{jLj'}W(j'l'jl;\tfrac{1}{2}L)Y_{l'}{}^{m_i+M-m_f}(\hat{p}_f)R_{LM}(M_i,M_f,\kappa,\kappa'), \tag{A14}$$

[12] M. E. Rose, *Relativistic Electron Theory* (John Wiley & Sons, Inc., New York, 1961).

where

$$R_{LM}(M_i,M_f,\kappa,\kappa')=(2L+1)i\omega\int\int r_N{}^2dr_N r_e{}^2dr_e\{j_L(\omega r_<)h_L{}^{(1)}(\omega r_>)J_{LM}(M_i,M_f,r_N)[f_\kappa\bar{f}_{\kappa'}+g_\kappa\bar{g}_{\kappa'}]$$
$$+(i/[L(2L+1)]^{1/2})j_{L-1}(\omega r_<)h_{L-1}{}^{(1)}(\omega r_>)I_{L,L-1,M}(M_i,M_f,r_N)[L(f_\kappa\bar{g}_{\kappa'}-g_\kappa\bar{f}_{\kappa'})+(\kappa-\kappa')(f_\kappa\bar{g}_{\kappa'}+g_\kappa\bar{f}_{\kappa'})]$$
$$+(i/[(L+1)(2L+1)]^{1/2})j_{L+1}(\omega r_<)h_{L+1}{}^{(1)}(\omega r_>)I_{L,L+1,M}(M_i,M_f,r_N)$$
$$\times[-(L+1)(f_\kappa\bar{g}_{\kappa'}-g_\kappa\bar{f}_{\kappa'})+(\kappa-\kappa')(f_\kappa\bar{g}_{\kappa'}+g_\kappa\bar{f}_{\kappa'})]\},\quad\text{(A15)}$$

where bars are again used to denote final-state values and $r_>$, $r_<$ are the greater and lesser of r_N, r_e. The expression for the amplitude for a magnetic multipole transition is similar in form to that above and not given explicitly here.

The differential cross section for a pure electric multipole transition of order L, when the electron beam is unpolarized and the target nuclei unaligned, is given in terms of the amplitudes by

$$\sigma(\theta)=\left(\frac{1}{2\pi}\right)^2V^2\frac{p_f}{p_i}E_iE_f\frac{1}{2(2I_i+1)}\times\sum_{\substack{M_i,M_f,\\ m_i,m_f,M}}|E_{LM}(M_i,M_f,m_i,m_f,\mathbf{p}_i,\mathbf{p}_f)|^2,\quad\text{(A16)}$$

where θ is the angle between $\mathbf{p}_i$ and $\mathbf{p}_f$ (the scattering angle). A useful measure of the strength of the transition is given by the reduced transition probability, $B(EL)$, defined by

$$B(EL)\equiv\frac{1}{(2I_i+1)}\times\sum_{MM_iM_f}\left|\int d^3r_Nr_N{}^LY_L{}^M(\hat{r}_N)\rho_N(M_i,M_f,\mathbf{r}_N)\right|^2.\quad\text{(A17)}$$

In the calculations presented in the main text only the first term of Eq. (A6) (the scalar term) is retained and evaluated in the long-wavelength limit ($\omega a<1$, where a is the nuclear radius). Further, the distortion due to the static Coulomb field of the nucleus, $V(r)$, is assumed to be the same in both initial and final states, and consequently the distinction denoted by bars in Eqs. (A5) and (A15) has been dropped. Advantage has been taken of the dependence of J_{LM} on M_i and M_f to write

$$J_{LM}(M_i,M_f,r_N)=C_{M_iMM_f}{}^{I_iLI_f}\rho_L(r_N),\quad\text{(A18)}$$

where $\rho_L(r)$ is the quantity which appears in Eq. (1) of the text. The sum over M_i and M_f in Eqs. (A16) and (A17) can now be performed explicitly to render[13]

$$\sigma(\theta)=(1/2\pi)^2V^2(p_f/p_i)E_iE_f\tfrac{1}{2}\times\sum_{m_i,m_f,M}|E_{LM}(m_i,m_f,\mathbf{p}_i,\mathbf{p}_f)|^2\quad\text{(A19)}$$

and

$$B(EL)=(2L+1)\left(\int r^L\rho_L(r)r^2dr\right)^2,\quad\text{(A20)}$$

where E_{LM} is given by Eq. (A14) having lost its dependence on M_i and M_f because R_{LM} reduces simply to an integral of the form:

$$R_L(\kappa,\kappa')=\int_0^\infty[f_\kappa f_{\kappa'}+g_\kappa g_{\kappa'}]C_L(r)dr,\quad\text{(A21)}$$

where the cutoff function is

$$C_L(r)=r^{L+2}\int_r^\infty\rho_L(r')r'^{-L+1}dr'+r^{-L+1}\int_0^r\rho_L(r')r'^{L+2}dr'.\quad\text{(A22)}$$

The evaluation of these integrals is discussed in I. Clearly $C_L(r)\sim r^{-L+1}$ outside the nucleus ($\rho_L(r)\to 0$), and for angular momentum components for which κ, $\kappa'>p_ia$, the contribution to the integral of the interior region may be neglected and R_L approximated by the "point nucleus" expression,

$$R_L(\kappa,\kappa')\simeq\int(f_\kappa f_{\kappa'}+g_\kappa g_{\kappa'})r^{-L+1}dr,\quad\text{(A23)}$$

which can be expressed in a closed form.[14]

In order to investigate the effect of neglecting, in the expression for the cross section, the current terms in Eq. (A6), a specific nuclear model is considered. The model is the inhomogeneous charged liquid drop model which is assumed to vibrate with irrotational and incompressible liquid motion.[15] The transition charge and current densities, in this case, have multipole components given by

$$J_{LM}(M_i,M_f,r_N)=C_{M_fMM_i}{}^{I_fLI_i}\beta_Lr_N{}^{L-1}d\rho_0/dr_N,\quad\text{(A24)}$$
$$I_{JLM}(M_i,M_f,r_N)=\delta_{J,L+1}C_{M_fMM_i}{}^{I_fLI_i}(-i\omega)\beta_L\times[(2L+1)/L]^{1/2}r_N{}^{L-1}\rho_0,\quad\text{(A25)}$$

where ρ_0 is the equilibrium charge density. Eq. (A24) together with Eq. (A18) give Eq. (3) in the text; the effect of including I_{JLM} is investigated here. It can be shown directly that, in the *Born approximation*, the effect of including the current terms, in this case, is to introduce a simple angular-dependent factor in the

[13] The corresponding expression in I, Eq. (2.13), is missing a factor of $\frac{1}{2}$.

[14] J. T. Reynolds, D. S. Onley, and L. C. Biedenharn, J. Math. Phys. **5**, 411 (1964).

[15] L. J. Tassie, Australian J. Phys. **9**, 407 (1956).

cross section:

$$[\sigma(\theta)]_{\text{charge+current}} = F(\theta)[\sigma(\theta)]_{\text{charge only}}. \quad \text{(A26)}$$

Explicitly,

$$F_L(\theta) = \left[1-\left(\frac{\omega}{q}\right)^2\right]^2 + \left(\frac{\omega}{q}\right)^2\left(\frac{L+1}{L}\right) \times \frac{q^2[E_iE_f - m^2 - p_ip_f\cos\theta] + p_i^2p_f^2\sin^2\theta}{q^2[E_iE_f + m^2 + p_ip_f\cos\theta]}, \quad \text{(A27)}$$

where $q=q(\theta)$ is the momentum transfer in the collision. As is easily seen, under conditions for which $m_e,\ \omega \ll E_i$, this factor is essentially unity except in the extreme forward and backward directions. Although, as has been pointed out, the Born approximation is not an accurate approximation over the complete range of θ considered, the above result should permit the conclusion that the effect of these current terms is negligible over this range, even at the minima of the form factors.

PHYSICAL REVIEW VOLUME 134, NUMBER 5B 8 JUNE 1964

Fission Barrier of Thallium-201

DONALD S. BURNETT,* RAYMOND C. GATTI, FRANZ PLASIL, P. BUFORD PRICE,†
WLADYSLAW J. SWIATECKI, AND STANLEY G. THOMPSON
Lawrence Radiation Laboratory, University of California, Berkeley, California

(Received 23 December 1963)

A new method involving the detection of fission fragments in mica has been applied to the measurement of the fission cross section of the compound nucleus Tl^{201} produced by bombardments of Au^{197} with helium ions. These data have been interpreted in terms of an expression for the ratio of fission to neutron-emission probabilities similar to those used conventionally, but modified to include the effect of quantum-mechanical barrier penetrability. In this way a height of 22.5±1.5 MeV was found for the fission barrier of Tl^{201} and a lower limit on the width could be established. The above value of the barrier, when interpreted on the basis of the liquid-drop theory, leads to an accurate determination of the ratio of the electrostatic to the surface energy of nuclei. This serves to establish the constant of proportionality between the "fissionability parameter" x and the value of Z^2/A as follows: $x=(Z^2/A)/(48.4\pm0.5)$. This measured barrier height, when added to the ground-state mass of Tl^{201}, gives a saddle-point mass of this nucleus equal to 200.9949±0.0015 mass units (carbon scale).

I. INTRODUCTION

THE primary purpose of this work was determination of the fission barrier of the compound nucleus Tl^{201} produced by bombardment of Au^{197} with helium ions. The interest in reliable measurements of fission barriers is twofold. First, barrier heights are among the most fundamental and, at the same time, the simplest predictions of a theory of fission. In particular, within the framework of the liquid-drop model, accurate theoretical values of relative barrier heights have become available recently.[1,2] Most of the experimental information on fission barriers has so far been confined to the heavy-element region, where the barrier heights are only a few MeV, and the relative size of corrections due to shell effects is almost of the same order of magnitude.[3,4] As a result, the interpretation of the poor agreement between experiment and the simple liquid-drop theory is difficult in this region of the periodic table. The situation could be clarified by an extension of barrier measurements to the lighter elements below lead, where the barrier heights are expected to increase rapidly to 20 MeV and more.

The second reason for the importance of fission barrier measurements is in connection with the determination of adjustable constants in semiempirical mass formulas.[5] The measurement of a fission barrier, equivalent to the measurement of the mass of a nucleus in its distorted "saddle-point configuration," is potentially the most accurate way of determining the ratio of the nuclear surface tension to the electrostatic energy. The limited use made so far of fission barrier measurements in fitting constants in semiempirical mass formulas is probably due to the inadequate understanding of fission barrier systematics in the heavy-element region. A clarification by barrier measurements for lighter elements would reduce these uncertainties and would add considerably to the understanding of the systematics of nuclear masses in general.

* Present address: Kellogg Radiation Laboratory, California Institute of Technology, Pasadena, California.

† Present address: General Electric Company, Schenectady, New York.

[1] V. M. Strutinski, N. Ya Lyashchenko, and N. A. Popov, Zh. Eksperim. i Teor. Fiz. **43**, 584 (1962)[English transl.: Soviet Phys.—JETP **16**, 418 (1963)].

[2] S. Cohen and W. J. Swiatecki, Ann. Phys. (N. Y.) **22**, 406 (1963).

[3] W. J. Swiatecki, Phys. Rev. **101**, 97 (1956).

[4] Sven A. E. Johansson, Nucl. Phys. **22**, 529–552 (1961).

[5] W. J. Swiatecki, in *Proceedings of the Second International Conference on Nuclidic Masses*, edited by W. Johnson, Jr. (Springer-Verlag, Vienna, 1963).